

Example-Driven Landmarking of Human Body Scans

DongWook Yoon, Nambin Heo, Hyeong-seok Ko,
Seoul National University, Seoul, South Korea.

Keywords: 3D body scan, anthropometric landmarks, human body measurements

Introduction

Every human body is different. Although variations in physical characteristics are observed across entire body, the clothing community has abstracted this diversity into a discrete, tractable set of prominent points termed *body landmarks* (BLs). BLs can be identified by visual examination or palpation. For example, the belly button is a prominent feature in the abdomen, and the cervical is the surface point at the seventh vertebra of the spine. As BLs compactly summarize body shape, identification of BLs is of fundamental significance in clothing production. This paper proposes a new technique for identifying BLs in a given human body scan.

The task of identifying the BLs of a particular subject based on his or her scanned geometry can potentially be facilitated by considering data from a population in whom BLs have been identified and three-dimensional (3D) body geometries have been scanned. Several body scanning/measurement projects have been conducted worldwide (e.g., CAESAR, Size USA, and Size Korea), and some studies have produced data packages consisting of a set of 3D-scanned bodies along with annotated BLs. We will term such a package *landmarked population*. The goal of this work was to develop a technique to landmark a newly scanned body based on landmarked population.

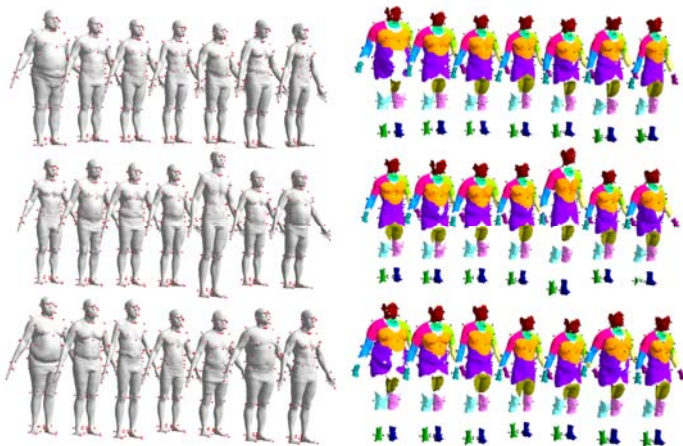


Figure 1: (a) The landmarked population, (b) Decomposition of the population into part-meshes (Among 1025 individuals, only 21 are shown).

Our utilization of a landmarked population is based on both the landmark-surface dependency principle and the locality principle. The *landmark-surface dependency principle* states that, for example, when two upper arms belonging to two different individuals are identical, the BLs of the two upper arms should be identical. Although it is possible that skeletal structures are not identical, the rationale behind the principle is that, when skeletal discrepancy is not evident, we have no choice but to rely on available

surface data. In this work, when the shapes of two body parts of two different subjects are similar, we assume that their landmarks are similar.

The *locality principle* states that BLs of distant body parts (of the same person) are not necessarily related. The principle implies that, for example, landmarking of an arm does not need to be performed in close association with landmarking of a leg. In this work, if the surface geometries of two arms (belonging to two different individuals) are identical, even if other body part surfaces are not identical, we assume that arm BLs are identical.

For any given unmarked body, our example-driven landmarking technique searches the closest match in the landmarked population and applies the landmarks of the matched individual to the unmarked body. This is an application of the landmark-surface dependency principle. The locality principle tells us that the search need not to be performed over entire bodies but can be performed over each body part termed *part-mesh*. We call this *part-wise matching*.

Body Segmentation

Decomposing the body into portions that are too large conflicts with the locality principle. However, a part-mesh should be sufficiently large to establish the matching context. Based on the above considerations, we decompose a human body into 16 parts as shown in Figure 1. Some part-meshes may overlap at boundaries, and the part-meshes may not entirely cover the body mesh. We accept these imperfection because they helps us to find the best match. Inclusion of unnecessary mesh portions can hinder this process; some overlapping portions are included to provide necessary matching context. Our automatic body segmentation requires establishment of correspondence across different bodies. The correspondence problem can be stated as follows: if there are two human bodies *A* and *B*, which surface point on body *B* corresponds to a marked point *x* on body *A*? Establishment of this correspondence is termed the *parameterization*. In this work, we employ the mesh transformation of Allen and colleagues [1] for the landmarked population parameterization. Once parameterization is complete, the correspondence is established not only for BLs but for any arbitrary body points. We manually decomposed the only one standard body. Part-meshes for another body can be obtained as corresponding parts to the standard part-meshes. This approach enables segmentation of the entire (parameterized) population without human intervention.

Part-wise Matching

After preparation as described in the previous section, we now indicate how landmarking of a novel 3D scan body can be performed. The goal here is to find the best-matched landmarked part-meshes (LPMs) to the unmarked body *D* and to apply the landmarks thereof to *D*. This task involves aligning/scaling of an LPM around *D* and requires a metric that can measure match quality.



Figure 2: Best-matched LPMs aligned to *D*: (a) Unmarked scan body *D*, (b) Best-matched part-meshes, (c) Overlapping of (a) and (b). The surface constructed by the best-matched part-meshes aligns well with the unmarked body. The image demonstrates that the aligned part-meshes can provide an effective geometrical context for BL identification., (d) Landmarking result. Red points represent the reference BLs and green ones represent BLs identified using our technique.

A widely used mesh registration method for aligning/scaling an LPM to *D* is available. This is the iterative-closest-point(ICP) algorithm. For a given LPM, the ICP approach locates a translated/rotated/scaled version which reduces *matching error* introduced by Besl [2]. As a LPM matches well to *D*, corresponding matching error reduces accordingly. We obtain a set of best-matched part-meshes by selecting part-meshes with the lowest matching errors. Finally, best-matched part-meshes were projected onto the unmarked body to obtain the required landmarks.

Results and Conclusion

Experiments were performed using a Windows XP environments. Our method was embodied with Visual C++ and visualized with OpenGL API. We used 1025 landmarked bodies of CAESAR data for the experiments.

Table 1: Average landmarking errors in 250 subjects.

BL	error (mm)	BL	error (mm)
Sellion	6.69	Rt. Infraorbitale	5.60
Lt. Infraorbitale	6.37	Supramenton	5.49
Rt. Tragion	7.32	Rt. Gonion	11.34
Lt. Tragion	6.50	Lt. Gonion	8.44
Nuchale	16.01	Rt. Clavicale	6.56
Suprasternale	12.18	Lt. Clavicale	9.28
Rt. Thelion/Bustpoint	7.78	Lt. Thelion/Bustpoint	10.71
Substernale	9.84	Rt. 10th Rib	22.21
Rt. ASIS	32.97	Lt. 10th Rib	18.38
Lt. ASIS	34.52	Rt. Iliocristale	14.61
Rt. Trochanterion	14.71	Lt. Iliocristale	18.60
Lt. Trochanterion	14.39	Cervicale	11.87
10th Rib Midspine	13.91	Rt. PSIS	27.96
Lt. PSIS	28.40	Waist, Preferred, Post.	26.02
Rt. Acromion	21.17	Rt. Axilla, Ant	39.31
Rt. Radial Styloid	10.97	Rt. Axilla, Post.	21.87
Rt. Olecranon	7.90	Rt. Humeral Lateral Epicn	10.43
Rt. Humeral Medial Epicn	11.24	Rt. Radiale	9.04
Rt. Ulnar Styloid	7.51	Lt. Acromion	10.97
Lt. Axilla, Ant	30.14	Lt. Radial Styloid	7.29
Lt. Axilla, Post.	22.50	Lt. Olecranon	10.45
Lt. Humeral Lateral Epicn	7.48	Lt. Humeral Medial Epicn	11.32
Lt. Radiale	8.27	Lt. Ulnar Styloid	8.40
Rt. Knee Crease	6.86	Rt. Femoral Lateral Epicn	11.49

Rt. Femoral Medial Epicon	17.69	Rt. Lateral Malleolus	7.21
Rt. Medial Malleolus	6.77	Rt. Sphyrion	5.66
Rt. Calcaneous, Post.	13.95	Lt. Knee Crease	6.47
Lt. Femoral Lateral Epicon	9.00	Lt. Femoral Medial Epicon	15.97
Lt. Lateral Malleolus	6.08	Lt. Medial Malleolus	7.10
Lt. Sphyrion	8.27	Lt. Calcaneous, Post.	8.17
Crotch	23.68	Overall average	13.43

The landmarking accuracy of the proposed method was tested as follows. We chose one individual (termed the *subject*) among the 1025 individuals, and regarded the remaining 1024 individuals as the population. We considered the (known) landmarks of the subject to reflect perfect measurement accuracy, but temporarily ignored these data to seek to landmark the subject using our novel procedure. We compared our data with the real values. Landmarking error was measured by the Euclidian distance between the procedurally obtained landmark and the real datum. The test described above was performed on 250 individuals. The mean landmarking error of the proposed technique was about 1.34cm. Considering that the acceptable error of the most traditional measurements is about 1cm [3], the landmarking error of our new technique is reasonable.

The ICP approach was applied to part-wise matching. However, there are several advanced mesh registration techniques [4, 5] which we plan to exploit to improve both accuracy and convergence.

Acknowledgment

This work was supported by the Brain Korea 21 Project in 2009, Seoul Metropolitan Government R&BD Program (10581), Ministry of Culture Sports and Tourism, ASRI (Automation and Systems Research Institute at Seoul National University), and Ministry of Science and Technology under National Research Laboratory (NRL) grant M10600000232-06J0000-23210.

References

- [1] B. Allen, B. Curless, and Z. Popovic (2003). The space of human body shapes : reconstruction and parameterization from range scans. ACM Transactions on Graphics, Proc. ACM SIGGRAPH 2003, 22(3):587-594.
- [2] P.J. Besl and N.D. McKay (1992). Method for registration of 3-D shapes. IEEE Transactions on Pattern Analysis and Machine Intelligence, 14(2), 239-256.
- [3] Zouhour Ben Azouz, Chang Shu and Anja Mantel (2006). Automatic locating of anthropometric landmarks on 3D human models. Proceedings of the Third International Symposium on 3D Data, 750-757.
- [4] A. Johnson and M. Hebert (1997). Surface registration by matching oriented points. Proc. of Int. Conf. Recent Advances in 3-D Digital Imaging Modeling, 12-15.
- [5] Sotiris Malassiotis and Michael G. Strintzis (2007). Snapshots: A novel local surface descriptor and matching algorithm for robust 3D surface alignment. IEEE Transactions on pattern analysis and machine intelligence, 29(7):1285-1290.